This is the accepted manuscript made available via CHORUS. The article has been published as:

Interplay between strong correlations and electronic topology in the underlying kagome lattice of math xmlns="http://www.w3.org/1998/Math/MathML">mrow>msub>mi>Na/mi>mrow>mn>2/mn>mo>//mo>mn>3/mn>/mrow>/msub>mi>Co/mi>msub>mi mathvariant="normal">O/mi>mn>2/mn>/msub>/mrow>/math>

I. F. Gilmutdinov, R. Schönemann, D. Vignolles, C. Proust, I. R. Mukhamedshin, L. Balicas, and H. Alloul

Phys. Rev. B **104**, L201103 — Published 5 November 2021

DOI: 10.1103/PhysRevB.104.L201103

Interplay between strong correlations and electronic topology in the underlying kagome lattice of $Na_{2/3}CoO_2$.

I.F. Gilmutdinov[1,4], R. Schönemann[2], D. Vignolles[1], C. Proust[1], I.R. Mukhamedshin[3,4], L. Balicas[2] and H. Alloul[3]

[1] Laboratoire National des Champs Magnétiques Intenses, 31400 Toulouse, France.

[2] National High Magnetic Field Lab, Florida State University, Tallahassee, Florida, 32310 USA

[3] Université Paris-Saclay, CNRS, Laboratoire de Physique des Solides, 91405, Orsay, France.

[4] Institute of Physics, Kazan Federal University, 420008 Kazan, Russia

Abstract

Electronic topology in metallic kagome compounds is under intense scrutiny. We present transport experiments in $Na_{2/3}CoO_2$ in which the Na order differentiates a Co kagome sub-lattice in the triangular CoO_2 layers. Hall and magnetoresistance (MR) data under high fields give evidence for the coexistence of light and heavy carriers. At low temperatures, the dominant light carrier conductivity at zero field is suppressed by a *B*-linear MR suggesting Dirac like quasiparticles. Lifshitz transitions induced at large *B* and *T* unveil the lower mobility carriers. They display a negative B^2 MR due to scattering from magnetic moments likely pertaining to a flat band. We underline an analogy with heavy Fermion physics.

Introduction: The influence of frustration of exchange on the magnetic properties of transition metal compounds has been investigated thoroughly in spin structures. The Herbertsmithite compound, whose Cu^{2+} sites are ordered in a two-dimensional kagome structure, is considered as a good reference for a Quantum Spin Liquid, as no spin ordering has been detected in its ground state (1).

Attempts to synthesize doped metallic states in this kagome system by chemical substitutions have been so far unsuccessful (2). Those were motivated by a search for superconductivity in the phase diagram but also by an analogy with the honeycomb lattice such as that of graphene in which Dirac points are located (3). Local Density Approximation (LDA) calculations for a single orbital per site in weakly correlated kagome lattices also show the presence of Dirac or Weyl points as well as flat electronic bands (4). One wonders how such topological states would evolve in the presence of strong correlations. This led intensive searches for correlated kagome compounds e.g. in *3d* stannite materials like FeSn (5), CoSn (6) or $Co_3Sn_2S_2$ (7).

Here, we present an alternative approach based on the Na cobaltate compounds Na_xCoO_2 where the Co atoms are ordered on a triangular lattice. The originality of this system has been revealed by earlier NMR/NQR experiments. It was shown that the Na located between the CoO_2 layers (Fig. 1a) displays distinct orderings depending on the Na content (8) (9). The electrostatic incidence of the Na^+ ionic order induces a charge disproportionation of the Co sites (10). This has been evidenced in great detail in the case of the x=2/3 phase (11) (12) (13) in which a subset of Co sites remain in a Co^{3+} state with filled non-magnetic t_{2g} orbitals (Fig. 1b) while the complementary set of Co sites are ordered in a kagome sub-lattice having delocalized charge carriers (Fig. 1d). LDA calculations indicate that the Na order yields the minimum energy state for this compound (14), while LDA+U computations (15) demonstrate that a large coulomb interaction U is required to induce the disproportionation of the Co sites.

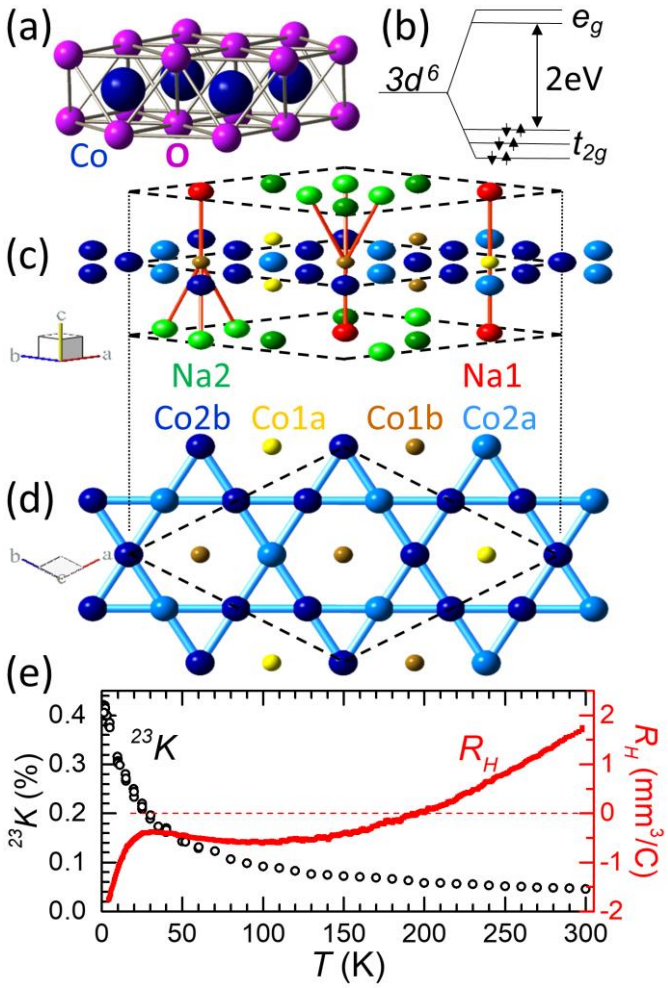


Fig. 1. (a) Structure of an isolated CoO_2 layer. (b) Splitting of the Co *3d* levels induced by the crystal field in Na_xCoO_2 for x=1. (c) Differentiation for x=2/3 of the Co sites induced by the ordered stacking of Na above and below the CoO_2 layer. (d) 2D arrangement of the two types of sites in the Co plane (11). The ^{59}Co NMR shift data gave evidence that Co1a and Co1b (yellow and brown) are non-magnetic Co^{3+} sites with filled t_{2g} levels as in (b). The *3d* orbitals of the Co2a and Co2b sites (light and dark blue) arranged in a kagome sub-lattice are both nearly identically involved at the Fermi level(10) (16). (e) The ^{23}Na NMR shift ^{23}K (left scale) monitors the spin susceptibility on those sites (associated with the hole doping of the correlated electronic bands of their kagome structure). It displays a Curie-Weiss like T dependence (17) below 30 K concomitantly with the anomalous increase in magnitude of the Hall constant R_H (right scale) (18).

Early experiments performed on samples with Na content near x=2/3 have indeed revealed singularly large values of the magnetic susceptibility (17) (19), specific heat(20) (21) and of T^2 dependence of the resistivity (22) which are obvious signs of strong electronic correlations. NMR shift measurements on the various Na and Co nuclear sites have given evidence

that the local spin susceptibility χ of the Co2a and Co2b sites forming the kagome sub-lattice displays a large increase below 30 K (Fig. 1e), with respect to phases with a different Na content. Meanwhile, μSR experiments do not provide evidence for static magnetic order down to 0.1 K(23). Hence the local χ reaches a constant value only below T=1.5 K(17).

We have recently synthesized(24) high quality single crystals of the Na ordered $Na_{2/3}CoO_2$ phase with large residual resistivity ratios RRR=R(300 K)/R(1.5 K)~200. A change in the sign of the Hall-effect at 200 K was found to be followed below 30 K by a reproducible and unexpected large increase(18) in its negative magnitude (Fig. 1e). These modifications of the electronic properties indicate that the reconstruction of the Fermi Surface (FS) which occurs already above 200 K is followed by a large increase in electronic carrier mobility below 30 K.

Those results therefore underscore the need to perform detailed low T band structure (BS) and FS studies on this specific kagome lattice material. As quantum oscillations (QOs) were discovered in uncontrolled quality samples(25) we have done high field measurements on our high-quality single crystals. We did not find QOs immediately in this phase but disclosed a series of new unexpected behaviors in the transport data.

We shall detail hereafter that an applied field of ~30 T in the ground state induces a change in the sign of the Hall effect, implying a major change in the electronic properties. We shall then underline the contrasting behavior of the magnetoresistance (MR) which changes sign and field dependence for increasing T. The negative B^2 dependence of the MR attributable to heavy carriers will be assigned to paramagnetic spin scattering in analogy to similar observations in the Heavy Fermion compounds. Comparisons with the multiband BS known for kagome compounds will lead us to suggest that the B linear MR of the mobile carriers could be associated with Dirac/Weyl linear dispersing bands. In this peculiar metallic kagome compound the band structure topology therefore retains singular behaviors in the presence of strong correlations.

Experimental results

***Hall effect*:** Transport data was taken on a series of distinct samples and in two different high magnetic field facilities as detailed in the Supplemental Material (26). The small residual resistivity (~2 $\mu\Omega\cdot$cm) measured in our single crystals proves the low level of disorder for this x=2/3 phase. In preliminary studies done above 2 K the Hall resistivity ρ_{xy} was found to be

linear in B below 9 T(18). But, when searching for QO at T=0.35 K under high magnetic fields at the Maglab in Tallahassee, we found that ρ_{xy} goes through a minimum at ~15 T, and *becomes positive above 30 T* as displayed in Fig. 2a.

This drastic non-linear behavior only moderately changes when the temperature is increased up to T=5 K. Then ρ_{xy} progressively becomes linear in B and remains negative above 30 K within the experimental field range. Our extensive data set for the Hall constant R_H (26) are summarized in the Fig. 2b. It provides evidence that R_H is nearly T and B independent up to 1.5 K and 12 T but abruptly changes its sign above ~30 T and levels off at a positive value at the highest fields

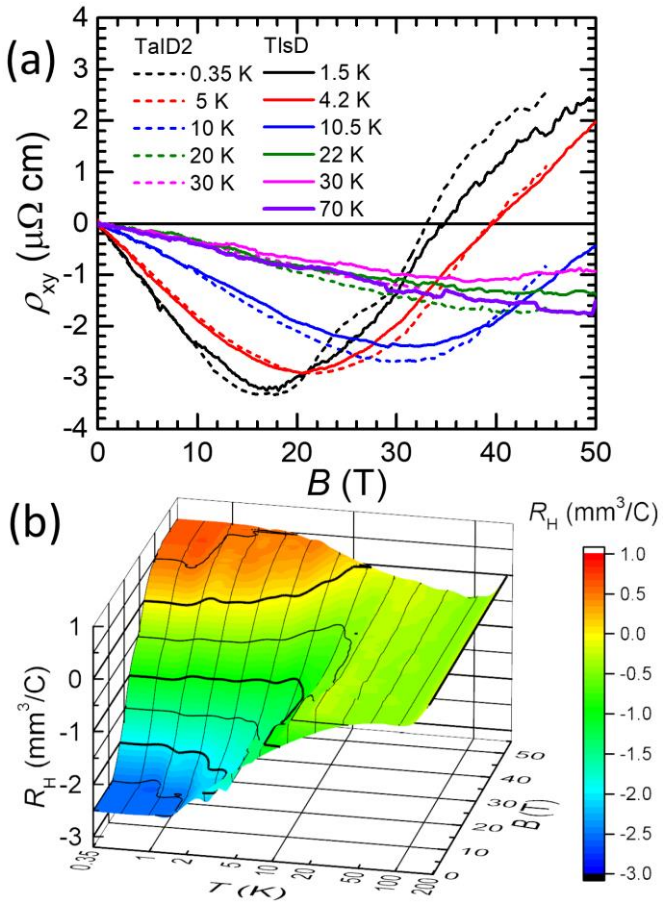


Fig. 2. (a) Hall resistivity ρ_{xy} as a function of $B=\mu_0 H$ at various T taken under DC applied fields H for sample TalD2 and under pulsed fields for sample TlsD agrees perfectly. (b) The full dataset described in (26), section II are displayed as a 3D plot of the Hall constant R_H versus B and T (log scale). R_H becomes positive under large fields for T<10 K, while the low field behavior of Fig. 1e is seen to saturate below 1.5 K at its lower negative value (26).

This abrupt sign change of R_H beyond 30 T implies a sharp reduction in electronic carrier density and/or mobility. So, assuming a Landé factor g=2, a Zeeman energy $g\mu_B B$~2 meV is sufficient to switch the transport from electron to hole-like carriers. On the contrary, the low field R_H remains negative up to 200 K so that the electrons remain dominant well beyond 30 K. These results demonstrate that thermal and Zeeman energies have distinct incidences on the transport.

Magnetoresistance: In the first search for Shubnikov de Haas effect at T=0.35 K we did not find any indication for QOs at high frequencies which would be associated with large FS pockets. But as shown in Fig. 3a an unexpectedly large positive MR was detected (~100% at 10 T and 800 % at 45 T). At T=0.35 K it exhibits an initial *linear in field behavior*, while above 5 K it becomes *negative and follows a B^2 dependence*.

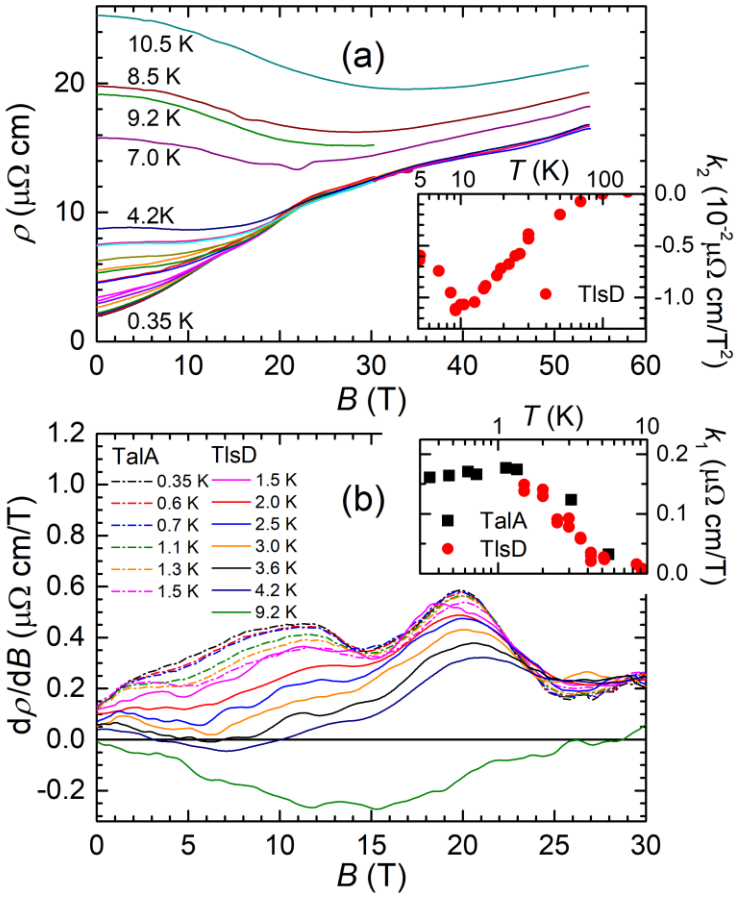


Fig.3 (a) Selected $\rho(B)$ curves taken from 0.35K to 1.5K for TalA sample and from 1.5K to 10.5K for TlsD. Details are available in (26), sec. II. (b) $d\rho(B)/dB$ displays maxima at 12T below 1.5K and at 20T below 5K. Insets: in (a) high T variation of the negative coefficient k_2 of the B^2 MR including data above 10K detailed in (26), sec. II. (b) Low T variation of the linear coefficient k_1 of the MR (see also (26), sec. V).

Other unusual behaviors also appear as the large *T* variation of $\rho(B,T)$ displayed for *B*=0 T disappears up to 1.5 K for fixed field *B*>12 T and even up to 5 K for fixed *B*>20 *T*. Those two fields also appear as slight steps in $\rho(B)$ seen as maxima in the $d\rho(B)/dB$ curves of Fig. 3b. There the maximum at 20 T is seen for *T* up to 5 K, while the one at 12 T disappears above 1.5 K. These derivative curves were found to be astonishingly reproducible on distinct sample batches (26).

The similar drastic loss of the ground state conductivity $\sigma=\sigma_{xx}$ which occurs beyond 20 T or beyond 5 K is illustrated in the 3D representation shown in Fig. 4. There σ is shown in a logarithmic scale versus *B* and *T*, with the latter also on a log scale. The corresponding linear representation of σ is displayed in (26) where it is shown that for this kagome phase $\sigma \sim \rho^{-1}$. In Fig. 4, the absence of *T* dependence of ρ below 5 K for *B*>20 T is illustrated by the constant field curves in the yellow range.

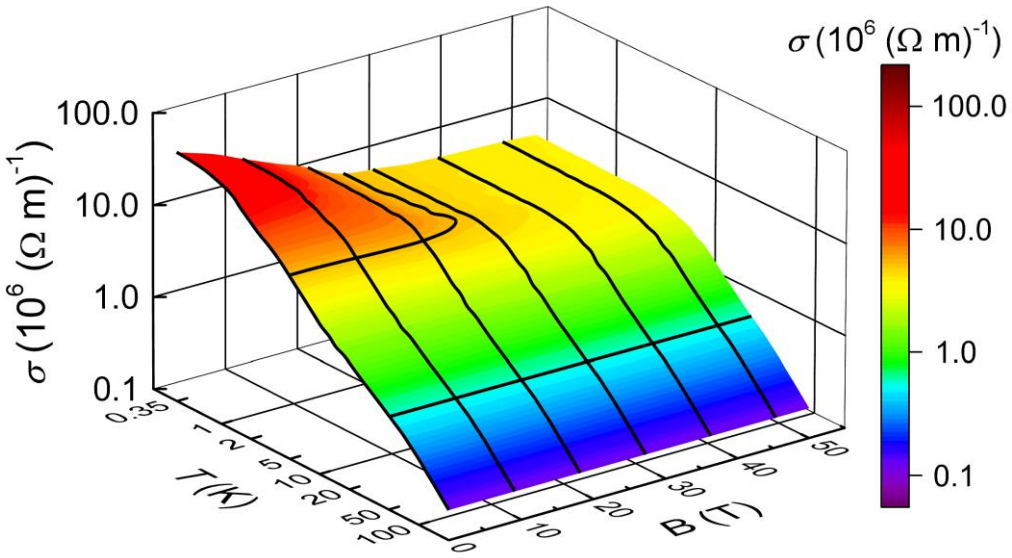


Fig. 4: 3D plot of the conductivity $\sigma(B,T)$ on a logarithmic scale highlighting the large increase which occurs below 5 K under small applied fields *B*<20 T. Here, data have been displayed up to T=100 K (log scale).

Ground state multiband data analysis

The minimal model one might use to analyze the low *T* data is a two-band model with hole and electron carriers at the Fermi level. For weakly interacting electrons in semiconductors or semi-metals(27) with quadratically dispersing bands the conductivities are $\sigma_h=n_h e\mu_h$ and $\sigma_e=n_e e\mu_e$ (where n_h, n_e,

μ_h and μ_e are the hole and electron carrier densities and mobilities). The classic equations for the conductivity and Hall constant, taking into account the Lorentz force acting on the carriers are(28):

$$\sigma = \frac{\sigma_h}{1+\mu_h^2 B^2} + \frac{\sigma_e}{1+\mu_e^2 B^2} \quad (1)$$

$$R_H = \frac{1}{e n_H} = \left[\frac{\sigma_h \mu_h}{1+\mu_h^2 B^2} - \frac{\sigma_e \mu_e}{1+\mu_e^2 B^2}\right] \sigma^{-2} \quad (2)$$

Measurements of σ, R_H and of the positive B^2 MR would allow us to extract the T dependencies of the carrier densities and mobilities assuming a charge neutrality condition. This approach has been found to hold even in some correlated metals such as the Fe pnictides(29).

In the present compound the NMR data implies a total number of 0.44 holes per Co atomic site of the kagome lattice, so eqs. (1) and (2) can be complemented by n_h-n_e=0.44. But this model does not explain the linear MR, which points towards singular band properties. We notice however in Fig. 4 that in the low T range the applied field B suppresses the conductivity of the high mobility electronic carriers and discloses that of the hole carriers. Therefore in the T=0 B~0 ground state for which the Hall effect remains constant σ splits into two contributions σ_e = 40.10^6(Ω m)$^{-1}$ and σ_h=(1/4)σ_e. We can use there eqs. (1) and (2) with R_H=-2.5 mm^3/C that is n_H=0.26 per Co site of the underlying kagome lattice, which yields n_e~0.16, n_h=0.60 and μ_e/μ_h=15.

The main conclusion of this simple two band analysis in terms of "effective"(30) carrier concentrations and mobilities is that *the holes are heavy carriers*. But this model cannot explain the B-linear contribution to the MR and has many other shortcomings. For instance, the steps in $\rho(B)$ at 12 T and 20 T suggest the occurrence of successive Lifshitz transitions. One could consider that such transitions eliminate above 20 T all electron pockets from the FS. But in Fig. 2 the variation of R_H with increasing B is smooth beyond 12 T and only changes sign above 30 T. This implies that at least an electron pocket remains above 20 T so that the multiband aspect persists in the high field range.

Magneto-transport properties as functions of *T*

The loss of conductivity seen up to 5 K in Fig 4 is concomitant with the large decrease of IR_HI and could be due to a mobility decrease for some of

the electronic pockets. One should distinguish the initial increase of $\rho(B=0)$ thermally driven by ground state excitations from its evolution beyond 5 K.
Fermi liquid properties: As can be seen in Fig. 4, the zero-field conductivity decreases rapidly with increasing T. We show in section IV of (26) that $\rho(T)=\rho_0+A\ T^2$ up to T=1.5 K, with similar A values for samples with slightly different ρ_0 values. Such a variation had been seen as well on a less characterized sample in which the x=2/3 ordered phase was apparently dominant(22). In a single band approach this had been interpreted as Fermi liquid behavior with a T^2 electron-electron scattering rate. Here, although many bands contribute to σ, we may conclude that the Fermi liquid scenario applies to the highly mobile electrons which dominate the transport at low temperatures. But beyond 20 T, under a fixed field σ becomes T independent up to 5 K while heavy carriers dominate the conductivity. Thus, these carriers display weaker intra-band scattering than the high mobility electrons. As we found (26) that the $T=0$ resistivity for B>20 T is sample independent, their mobility might then be governed by an intrinsic process such as a quantum inter-band scattering (31).

Magnetoresistance: We can clearly see in Fig. 3 the linear in B contribution to the MR which appears in the $B=0$ limit of the isothermal $d\rho/dB$. Fits of the data up to 5 T with a second order polynomial dependence $\rho(B,T)=\rho_0(T)+k_1B+k_2B^2$ shows that k_1 decreases with increasing T and vanishes for T~5 K as seen in the inset of Fig. 3b. This linear contribution is therefore intrinsically related to the conductivity of the high mobility electronic carriers. On the contrary beyond 5 K the MR is dominated by the negative k_2B^2 contribution and $d\rho/dB$ becomes B-linear in Fig. 3b. This MR detected upon suppression of the mobile electron conductivity is therefore associated with the heavy carriers. The reproducibility of k_1 and k_2 data displayed in section IV of (26) for distinct samples allows us to underline that those MR coefficients are intrinsic to the clean metallic phase.

Discussion

We have disclosed here a large contrast in the transport properties among the various carrier bands in $Na_{2/3}CoO_2$. The local Curie Weiss like susceptibility (Fig. 1e) has previously established the existence of large electronic correlations in the underlying Co kagome band structure. A hallmark of this behavior is the negative quadratic MR due to spin scattering, usually absent in weakly correlated materials.

The reproducibility of the NMR and transport data (26) allows us to exclude *a priori* disorder or extrinsic impurities for this local moment behavior. This negative MR is mostly effective on the low mobility carriers and is therefore reminiscent of the situation encountered in some Heavy Fermion Kondo lattice compounds. There the loss of coherence of the 4*f* Kondo electrons influence the transport governed by the *5d* bands (32). Here, the interplay stands between bands built from the multiplet of Co 3*d* sublevels. A similar proposal has been done for Hund differentiated Fe pnictides. (33)

This analogy in the incidence of the magnetic scattering contrasts however with the difference in most other magneto-transport properties. In the tetragonal 122 Fe pnictide the multiband analysis could be performed and matched with ARPES experiments (29), while quite weak magnetic contributions to the MR were detected (34). The $Na_{2/3}CoO_2$ metal surprisingly does not superconduct at low *T* and displays a series of original transport behaviors which have been so far individually observed in specific materials. The linear MR is usually associated with linear dispersing bands, partial filling of the lowest Landau level of small FS pockets or kinks in the Fermi surface (35). The detected steps of the conductivity imply the occurrence of low energy features near the Fermi level so that Lifshitz like transitions are observed upon moderate increases of *B* or *T*. The insensitivity to intrinsic disorder also raises fundamental questions about the respective incidences of intra and interband scattering.

An interpretation of these phenomena requires a specific investigation of the actual band structure of $Na_{2/3}CoO_2$ in which the kagome structure is certainly of major importance. We have indicated in (18) that ARPES experiments will be difficult to perform on the surface of Na ordered samples. As theoretical input is also still lacking, we may use as guidance the LDA calculations done for a single orbital per kagome lattice site. Those yield two conical Dirac bands and a flat band which cross at the Brillouin zone center (4). Such bands have been disclosed by ARPES experiments in the metallic kagome materials known so far, such as the Co stannites (5)(6)(7) or the recently discovered AV_3Sb_5 (A=alkali) (36). Therefore, it appears logical to anticipate that a similar situation occurs in the present case. With 0.44 hole per kagome site the Fermi level should occur within the flat band and the transport should depend markedly on the refined band structure modifications at the band crossing points.

As the conductivity of the large μ_e carriers is suppressed with a linear MR, one may speculate that those are associated with partially filled Dirac or Weyl linearly dispersing bands, for which a linear MR is expected (37).

The two steps suppression of these carriers with increasing *B* or *T* could indicate a slight energy splitting of the two conical bands. They would be depleted in turn by Lifshitz transitions due to chemical potential shifts that would disclose the low mobility carriers. The latter would then be associated with partly filled flat bands that are expected to display behaviors akin to localized states (38). One could alternatively wonder whether the mobile carriers could depart from their Fermi liquid behavior above the apparent Lifshitz transitions and become then incoherent and more localized.

To conclude we provided evidence indicating that topology, frustration, and correlated electron physics are entangled in this well characterized kagome material. Such an interplay has only been proposed to occur in few compounds. It is not blurred here by concomitant magnetic or structural phase transitions.

We hope that our results will stimulate realistic theoretical efforts including the role of Hund's and Spin Orbit couplings. Some of the open questions might as well be answered experimentally in future high field runs and through comparisons with the other kagome compounds.

Acknowledgements

We thank S. Benhabib for her help in experimental runs in LNCMI and acknowledge exchanges with A. Subedi, L. de Medici, M. Civelli, M-O. Goerbig, K. Behnia, B. Fauqué and V. Brouet. The crystal growth, XRD, low field magnetic and transport measurements were carried out at the Federal Center of Shared Facilities of Kazan Federal University. Travel of HA and IG between Orsay, Kazan and Toulouse has been financially supported by an "Investissement d'Avenir" allowance from the Labex PALM (No. ANR-10-LABX-0039-PALM). Collaborative work between HA and LB have been supported by an ICAM travel grant between Orsay and Tallahassee funded by the Gordon and Betty Moore foundation QuantEmX program.

L.B. is supported by the US-DOE, BES program through award DE-SC0002613. The National High Magnetic Field Laboratory is supported by the National Science Foundation through NSF/DMR-1644779 and the State of Florida. We also acknowledge support by the LNCMI-CNRS, member of the European Magnetic Field Laboratory (EMFL).

References

1. **P. Khuntia, M. Velazquez, Q. Barthelemy, F. Bert, E. Kermarrec, A. Legros, B. Bernu, L. Messio, A. Zorko, and P. Mendels,** Gapless ground state in the archetypal quantum kagome antiferromagnet $ZnCu_3(OH)_6Cl_2$, Nat. Phys. 16, 469 (2020)
2. **D. Guterding, H. O. Jeschke, and R. Valenti,** Prospect of quantum anomalous Hall and quantum spin Hall effect in doped kagome lattice Mott insulators, Scientific Reports 6, 25988 (2016)
3. **K. S. Novoselov, A. K. Geim, S. V. Morozov, D. Jiang, D., Zhang, S. V. Dubonos, I. V. Grigorieva, and A. A Firsov,** Electric Field Effect in Atomically Thin Carbon Films, Science 306, 666 (2004)
4. **I.I. Mazin, H. O. Jeschke, F. Lechermann, H. Lee, M. Fink, R. Thomale, and R. Valentı,** Theoretical prediction of a strongly correlated Dirac metal, Nat. Commun. 5, 4261 (2014)
5. **M. Kang, L. Ye, S. Fang, J-S. You, A. Levitan, M. Han, J. I. Facio, C Jozwiak , A. Bostwic, E. Rotenberg, M. K. Chan, R. D. McDonald, D. Graf, K. Kaznatcheev, E. Vescovo, D. C. Bell, E. Kaxiras, and J. Va,** Dirac fermions and flat bands in the ideal kagome metal FeSn, Nat. Materials 19, 163 (2020)
6. **M. Kang, S. Fang, L. Ye, H. C. Po, J. Denlinger, C. Jozwiak, A. Bostwick, E. Rotenberg, E. Kaxiras, J. G. Checkelsky, and R. Comin,** Topological flat bands in frustrated kagome lattice CoSn, Nat. Comm. 11, 4004 (2020)
7. **D. F Liu, A. J. Liang, E. K. Liu, Q. N.Xu, Y. W. Li, C. Chen, D. Pei, W. J Shi, S. K Mo, Kim, T. Dudin, C. Cacho, G. Li, Y. Sun, L. X. Yang, Z. K. Liu, S. S. P . Parkin, C. Felser, and Y. L. Chen,** Magnetic Weyl semimetal phase in a Kagomé crystal, Science 365, 1282 (2019)
8. **H. W. Zandbergen, M. Foo, Q. Xu, V. Kumar, and R. J. Cava,** Sodium ion ordering in Na_xCoO_2: Electron diffraction study, Phys. Rev. B. 70, 024101 (2004)
9. **H. Alloul, I.R. Mukhamedshin, G. Collin, and N. Blanchard,** Na atomic order, Co charge Disproportionation and Magnetism in Na_xCoO_2 for large Na content, Europhysics Lett. 82, 17002 (2008)
10. **I. R. Mukhamedshin, A. V. Dooglav, S. A. Krivenko, and H. Alloul,** Evolution of Co charge disproportionation with Na order in Na_xCoO_2, Phys. Rev. B. 90, 115151 (2014)
11. **H. Alloul, I. R. Mukhamedshin, T. A. Platova, and A. V. Dooglav,** Na ordering imprints a metallic kagome lattice onto the Co planes of $Na_{2/3}CoO_2$, Europhysics Lett. 85, 47006 (2009)
12. **T. A. Platova, I. R. Mukhamedshin, H. Alloul, A. V. Dooglav, and G. Collin,** Nuclear quadrupole resonance and x-ray investigation of the structure of $Na_{2/3}CoO_2$, Phys.Rev. B. 80, 224106 (2009)
13. **I. R. Mukhamedshin, and H. Alloul,** Na order and Co charge disproportionation in Na_xCoO_2, Physica B: Condensed Matter 460, 58 (2015)
14. **S. Meng, Y. Hinuma, and G. Ceder,** An investigation of the sodium patterning in Na_xCoO_2 by density functional theory methods, J. Chem. Phys., 128, 104708 (2008)
15. **Y. V. Lysogorskiy, S. A. Krivenko, I. R. Mukhamedshin, O. V. Nedopekin, and D. A. Tayurskii,** Origin of the electron disproportionation in the metallic sodium cobaltates, Phys. Rev. B. 94, 205138 (2016)

16. **I.R. Mukhamedshin, and H. Alloul,** ^{59}Co NMR evidence for charge and orbital order in the kagomé like structure of $Na_{2/3}CoO_2$. Phys. Rev. B. 84, 155112 (2011)
17. **I. R. Mukhamedshin, H. Alloul, G. Collin, and N. Blanchard,** ^{23}Na NMR Evidence for Charge Order and Anomalous Magnetism in Na_xCoO_2, Phys. Rev. Lett. 93, 167601 (2004)
18. **I. F. Gilmutdinov, I. R. Mukhamedshin, and H. Alloul,** Hall effect evidence for an interplay between electronic correlations and Na order induced band topology in Na_xCoO_2, Phys. Rev. Materials, 4, 044201 (2020)
19. **Maw Lin Foo, Yayu Wang, Satoshi Watauchi, H. W. Zandbergen, Tao He, R. J. Cava, and N. P. Ong,** Charge Ordering, Commensurability, and Metallicity in the Phase Diagram of the Layered Na_xCoO_2, Phys. Rev. Lett. 92, 247001 (2004)
20. **L. Balicas, Y. J. Jo, G. J. Shu, F. C. Chou, and P. A. Lee,** Local Moment, Itinerancy, and Deviation from Fermi-Liquid Behavior in Na_xCoO_2 for $0.71 \leq x \leq 0.84$. Phys. Rev. Lett. 100, 126405 (2008)
21. **M. Bruhwiler, B. Batlogg, S. M. Kazakov, C. Niedermayer, and J. Karpinski,** Na_xCoO_2 : Enhanced low-energy excitations of electrons on a 2d triangular lattice, Physica B 378, 630 (2006)
22. **S Y. Li, L. Taillefer, D. G. Hawthorn, M. A. Tanatar, J. Paglione, M. Sutherland, R. W. Hill, C. H. Wang, and X. H. Chen,** Giant Electron-Electron Scattering in the Fermi-Liquid State of $Na_{0.7}CoO_2$, Phys. Rev. Lett. 93, 056401 (2004)
23. **P. Mendels, D. Bono, J. Bobroff, G. Collin, D. Colson, N. Blanchard, H. Alloul, I. Mukhamedshin, F. Bert, A. Amato, and A. D. Hillier,** Cascade of Bulk Magnetic Phase Transitions in Na_xCoO_2 as Studied by Muon Spin Rotation. Phys.Rev. lett. 94, 136403 (2005)
24. **I. F. Gilmutdinov, I. R. Mukhamedshin, F. Rullier-Albenque, and H. Alloul,** Synthesis of sodium cobaltate Na_xCoO_2 single crystals with controlled Na ordering, J. Phys. Chem. Solids 121, 145 (2018)
25. **L. Balicas, J. G. Analytis, Y. J. Jo, K. Storr, H. Zandbergen, Y. Xin, N. E. Hussey, F. C. Chou, and P. A. Lee,** Shubnikov–de Haas effect in the metallic state of $Na_{0.3}CoO_2$, Phys. Rev. Lett. 97, 126401 (2006)
26. **I.F. Gilmutdinov, R. Schönemann, D. Vignolles, C. Proust, I.R. Mukhamedshin, L. Balicas, and H. Alloul,** Supplemental Material at [.....] for detalied data with evidence for reproducibility of the results.
27. **J. S. Kim, D. G. Seiler, and W. F. Tseng,** Multicarrier characterization method for extracting mobilities and carrier densities of semiconductors from variable magnetic field measurements, J. Appl. Phys. 73, 8324 (1993)
28. **H. Takahashi, R. Okazaki, Y. Yasui, and I. Terasaki,** Low-Temperature Magnetotransport of the Narrow-Gap Semiconductor $FeSb_2$. Phys. Rev. B. 84, 205215 (2011)
29. **F. Rullier-Albenque, D. Colson, A. Forget, and H. Alloul,** Hall effect and resistivity study of the magnetic transition, carrier content and Fermi liquid behavior in $Ba(Fe_{1-x}Co_x)_2As_2$. Phys. Rev. Lett. 103, 057001 (2009)
30. **F. Rullier-Albenque,** Influence of the Electronic Structure on the Transport Properties of Iron Pnictides. C. R. Phys. 17, 164 (2015)
31. **Y. Wang, H. P. Nair, N. J. Schreiber, J. P. Ruf, B.Cheng, D. G. Schlom, K. M. Shen, and N. P. Armitage,** Separated transport relaxation scales and interband

scattering in $SrRuO_3$, $CaRuO_3$, and Sr_2RuO_4 thin films, Phys. Rev. B 103, 205109 (2021)
32. **H.-H. Lai, S. E. Grefe, S. Paschen, and Q. Si,** Weyl-Kondo Semimetal in Heavy Fermion Systems, PNAS, 115, 93 (2018)
33. **F. Hardy, A. E. Bohmer, D. Aoki, P. Burger, T. Wolf, P. Schweiss, R. Heid, P. Adelmann, Y. X. Yao, G. Kotliar, J. Schmalian, and C. Meingast,** Evidence of Strong Correlations and Coherence-Incoherence Crossover in the Iron Pnictide Superconductor KFe_2As_2, Phys. Rev. Lett. 111, 027002 (2013)
34. **F. Rullier-Albenque, D. Colson, and A. Forget,** Longitudinal magnetoresistance in Co-doped $BaFe_2As_2$ and LiFeAs single crystals: Interplay between spin fluctuations and charge transport in iron-pnictides, Phys. Rev. B. 88, 045105 (2013)
35. **A. A. Abrikosov,** Quantum linear magnetoresistance. Europhys. Lett. 49, 789 (2000)
36. **B. R. Ortiz, S.l M. L. Teicher, Y. Hu, J. L. Zuo, P. M. Sarte, E. C. Schueller, A. M. M. Abeykoon, M. J. Krogstad, S. Rosenkranz, R. Osborn, R. Seshadri, L. Balents, J. He, and S. D. Wilson,** CsV_3Sb_5: AZ_2 Topological Kagome Metal with a Superconducting Ground State, Phys. Rev. Lett. 125, 247002 (2020)
37. **L. P. He, X. C. Hong, J. K. Dong, J. Pan, Z. Zhang, J. Zhang, and S. Y Li,** Quantum Transport Evidence for the Three-Dimensional Dirac Semimetal Phase in Cd_3As_2. Phys. Rev. Letters. 113, 246402 (2014)
38. **D. L. Bergman, C. Wu, and L. Balents,** Band touching from real-space topology in frustrated hopping models, Phys. Rev. B. 78, 125104 (2008)